16
Astrophysics and cosmology

Finite-temperature field theory finds extensive applications in astrophysical environments and cosmology. This chapter is devoted to an introduction to these applications. A more comprehensive discussion could easily fill whole books.

The end product of the evolution of any star is a white dwarf star, a neutron star, or a black hole, depending on the initial mass of the star. A white dwarf star is held up against gravitational contraction by electron degeneracy pressure (Section 16.1) whereas a neutron star is held up by baryon degeneracy pressure and repulsive baryon interactions (Section 16.2). The sun will end its days by swelling up into a red giant and then collapsing to a white dwarf. Neutron stars are formed in the gravitational collapse of stars with initial mass in the range from about two to eight solar masses. The collapse is sudden and may be seen as a supernova. The resulting star is initially quite warm, perhaps 10 to 40 MeV in temperature, but cools rapidly by neutrino emission (Section 16.3). If the initial mass of the dying star is too great then it will end as a black hole.

There was some excitement when it was realized that a first-order QCD phase transition about one microsecond after the big bang could influence the abundances of the light isotopes such as deuterium, helium, and lithium. However, quantitative calculations now show that this is very unlikely (Section 16.4); in addition QCD, with its known set of quark masses, probably does not undergo a first-order phase transition, as we saw in Chapter 10.

Going further back in time, it seems quite likely that the final baryon and lepton numbers of the universe were determined at around the electroweak temperature scale of 100 GeV. Sphaleron transitions were the last phenomena that were able to change these numbers (Section 16.5). Baryogenesis and leptogenesis may have originated at some much earlier epoch, in the context of grand unified or supersymmetric theories. It

379

may be that some very massive particles in such a theory preferentially decayed into baryons rather than antibaryons. The formation and decay rates of such particles are considered in Section 16.6.

16.1 White dwarf stars

A white dwarf is the end result of a star of about one solar mass after it has burned all its nuclear fuel. It is held up against gravitational collapse by the degeneracy pressure of electrons, although essentially all its mass is contributed by baryons. It is interesting to inquire to what extent the equation of state of the degenerate electron gas influences the structure of white dwarfs.

In a white dwarf, the pressure of the electrons dominates the pressure of the atomic nuclei while the mass density of the baryons dominates the total energy density. Therefore the energy density is approximately

$$\epsilon = \frac{m_{\mathrm{N}} n_e}{Y_e} \qquad (16.1)$$

where m_{N} is the nucleon mass, n_e is the electron density, and Y_e is the number of electrons per baryon. For a star composed predominantly of helium $Y_e = 1/2$, while for a star composed predominantly of iron $Y_e = 26/56$. These values follow from the requirement of electrical neutrality. There are small corrections due to the binding energy of the atomic nuclei and to their average kinetic energy.

To determine the mass and structure of cold, nonrotating, spherically symmetric stars, we use the Tolman–Oppenheimer–Volkoff equation from general relativity,

$$r^2 \frac{dP}{dr} = -G(\epsilon + P)(\mathcal{M} + 4\pi r^3 P)\left(1 - \frac{2G\mathcal{M}}{r}\right)^{-1} \qquad (16.2)$$

where

$$\mathcal{M}(r) = 4\pi \int_0^r \epsilon(r') r'^2 dr'$$

The function $\mathcal{M}(r)$ is the total mass contained within a sphere of radius r. We can neglect the pressure in comparison with the energy density. We can also neglect the general relativistic change in the metric. To an excellent approximation Newtonian gravitational physics applies.

It turns out that as the central density ϵ_{c} of the star increases, the mass increases at first while the radius decreases. As the central density is increased further, an asymptotic limit is reached for the stellar mass. White dwarfs with a mass greater than this "Chandrasekhar limit" cannot

exist. To understand this limit we recognize that at very high density the electrons become ultrarelativistic. The electron pressure for noninteracting electrons is then

$$P_e = \frac{\mu_e^4}{12\pi^2} \tag{16.3}$$

and the density is

$$n_e = \frac{\partial P_e}{\partial \mu_e} = \frac{\mu_e^3}{3\pi^2} \tag{16.4}$$

Together with (16.1) this results in the equation of state

$$P = K\epsilon^{4/3} \tag{16.5}$$

where K is a constant. This has the form of a polytrope (pressure proportional to the energy density raised to a power). Newtonian gravitational physics then predicts the unique asymptotic mass

$$M_\infty = 4.555 \left(\frac{K}{G}\right)^{3/2} = 5.735 Y_e^2 M_{\text{sun}} \tag{16.6}$$

where the second equality expresses it in terms of the mass of the sun [1]. This mass is independent of the central density and the radius, which is given by

$$R = 3.891 \left(\frac{K}{G}\right)^{1/2} \epsilon_{\text{c}}^{-1/3} = 4.20 \left(\frac{M_{\text{sun}}}{\epsilon_{\text{c}}}\right)^{1/3} Y_e^{2/3} \tag{16.7}$$

The physical constants used above are: the average nucleon mass $m_{\text{N}} = 0.939$ GeV; Newton's constant $G = 6.707 \times 10^{-39}$ GeV^{-2}; the solar mass $M_{\text{sun}} = 1.989 \times 10^{30}$ kg; and the solar radius $R_{\text{sun}} = 6.961 \times 10^8$ km. For a white dwarf composed of helium $M_\infty = 1.43 M_{\text{sun}}$. The Chandrasekhar limit is one of the fundamental concepts in astrophysics.

The story is not complete. When the electron density becomes high enough, roughly when $\mu_e = 5m_e$, electrons are captured by protons to form neutrons (the neutrinos escape from the star). The electron-to-baryon ratio Y_e decreases, and so does the mass. As a function of increasing central density the mass goes up, reaches a maximum just below the Chandrasekhar limit, and then decreases. When the star mass falls with increasing central density the star is gravitationally unstable and collapses further.

It is clear that several other more minor effects have been left out of this analysis. Among these is the change in the equation of state of the electron gas owing to interactions among the electrons. Let us see how important these interactions are. From our previous studies we know that

the first-order correction to the pressure in the limit $\mu_e \gg m_e, T$ is

$$P_e = \frac{\mu_e^4}{12\pi^2}\left(1 - \frac{3}{2}\frac{\alpha}{\pi}\right) \tag{16.8}$$

and the correction to the density is

$$n_e = \frac{\partial P_e}{\partial \mu_e} = \frac{\mu_e^3}{3\pi^2}\left(1 - \frac{3}{2}\frac{\alpha}{\pi}\right) \tag{16.9}$$

This means that the coefficient K is modified:

$$K \to K\left(1 - \frac{3}{2}\frac{\alpha}{\pi}\right)^{-1/3} \tag{16.10}$$

This changes the Chandrasekhar limit by only 0.2%. So, after all this hard work we find that the perturbative corrections in an ultrarelativistic electron gas are probably impossible to discern by measuring white dwarf masses and radii.

16.2 Neutron stars

A neutron star consists of almost pure neutron matter with a central density greater than that in atomic nuclei. This represent the final state in the evolution of many stars. Owing to their high central density, neutron stars serve as distant laboratories for the study of dense, relativistic, strongly interacting systems. Their central cores may have some component of hyperon matter or quark matter. Much theoretical work has been published on this topic over the last forty years. Here we can just touch on some of the important issues by studying a few illustrative theories of cold dense baryonic matter.

To first approximation the star consists of pure neutron matter. However, neutrons undergo beta decay by the process $n \to p + e^- + \bar{\nu}_e$. This decay will continue until the density of protons and electrons is high enough for the Pauli exclusion principle to prevent any further decays; this happens when the chemical potentials satisfy $\mu_n = \mu_p + \mu_e$. The neutrinos escape from the star. In fact, neutrino radiation is an important mechanism for the cooling of a neutron star from its initial temperature of 10 to 40 MeV following its birth by supernova. The details of neutrino cooling are a fascinating, and complicated, story in themselves. The interested reader is referred to Section 16.3 and to the bibliography at the end of the chapter.

As the central density increases, so does the baryon chemical potential. Eventually it becomes high enough that hyperons can be produced and coexist in chemical equilibrium with the neutrons and protons. The lowest

spin-1/2 baryon octet consists of $p, n, \Lambda, \Sigma^+, \Sigma^0, \Sigma^-, \Xi^0, \Xi^-$. If the baryon density is high enough, muons may appear too.

We will consider three different models for the equation of state. The first consists of relativistic but non-interacting neutrons. (It can be shown that the inclusion of noninteracting protons, whose abundance is determined by beta equilibrium with neutrons, does not modify the equation of state and therefore the structure of neutron stars by very much.) The second model consists of protons and neutrons in beta equilibrium, interacting via the exchange of σ, ω, and ρ mesons in the relativistic mean field approximation. The first two mesons heve been discussed already, in Chapter 11; the ρ meson is required here to reproduce the measured charge-symmetry energy of nuclear matter. The third model starts with the second and adds the six hyperons in the baryon octet. In addition, the vector meson ϕ is included, since it couples to the hyperons and represents vector repulsion among them.

All three models for the equation of state are based on the Lagrangian

$$
\begin{aligned}
\mathcal{L}_{\text{strong}} = \sum_j & \bar{\psi}_j (i\partial\!\!\!/ - m_j + g_{\sigma j}\sigma - g_{\omega j}\omega\!\!\!/ - g_{\phi j}\phi\!\!\!/ - g_{\rho j}\rho\!\!\!/^a T_a)\psi_j \\
& + \tfrac{1}{2}(\partial_\mu \sigma \partial^\mu \sigma - m_\sigma^2 \sigma^2) - \tfrac{1}{3}b m_{\text{N}}(g_\sigma \sigma)^3 - \tfrac{1}{4}c(g_\sigma \sigma)^4 \\
& - \tfrac{1}{4}\omega^{\mu\nu}\omega_{\mu\nu} + \tfrac{1}{2}m_\omega^2 \omega_\mu \omega^\mu - \tfrac{1}{4}\phi^{\mu\nu}\phi_{\mu\nu} + \tfrac{1}{2}m_\phi^2 \phi_\mu \phi^\mu \\
& - \tfrac{1}{4}\rho_a^{\mu\nu}\rho_{\mu\nu}^a + \tfrac{1}{2}m_\rho^2 \rho_\mu^a \rho_a^\mu
\end{aligned}
\tag{16.11}
$$

Here j runs over the spin-1/2 baryons in the octet and T^a is the isospin generator. The various models discussed above correspond to the inclusion or exclusion of some of the terms in $\mathcal{L}_{\text{strong}}$.

In the relativistic mean field approximation we allow the meson fields to acquire density-dependent average values; the nonzero ones are $\bar{\sigma}$, $\bar{\omega}_0$, $\bar{\phi}_0$, and $\bar{\rho}_0^3$. These are driven by the finite densities of particle number, baryon number, strangeness, and isospin asymmetry, respectively. From the Lagrangian, one can read off the effective baryon masses m_j^*,

$$
m_j^* = m_j - g_{\sigma j}\bar{\sigma}
\tag{16.12}
$$

and effective baryon chemical potentials μ_j^*,

$$
\mu_j^* = \mu_j - g_{\omega j}\bar{\omega}_0 - g_{\phi j}\bar{\phi}_0 - I_{3j}g_{\rho j}\bar{\rho}_0^3
\tag{16.13}
$$

where I_{3j} is the third component of the isospin of the jth baryon ($1/2$ for the proton, $-1/2$ for the neutron, etc.).

The particle densities are given in terms of the Fermi momenta by

$$
n_j = p_{\text{F}j}^3/3\pi^2
\tag{16.14}
$$

The Fermi momenta, in turn, are related to the effective chemical potentials by

$$\mu_j^* = \sqrt{m_j^{*2} + p_{\mathrm{F}j}^2} \qquad (16.15)$$

In a neutron star the matter is electrically neutral and in equilibrium under the strong, electromagnetic, and weak interactions. Chemical equilibrium among the baryons listed above, as well as the electrons and muons, implies the relations

$$
\begin{aligned}
\mu_p &= \mu_n - \mu_e & \mu_\Lambda &= \mu_n \\
\mu_{\Sigma^+} &= \mu_n - \mu_e & \mu_{\Sigma^0} &= \mu_n \\
\mu_{\Sigma^-} &= \mu_n + \mu_e & \mu_{\Xi^0} &= \mu_n \\
\mu_{\Xi^-} &= \mu_n + \mu_e &
\end{aligned}
\qquad (16.16)
$$

where $\mu_e = \sqrt{m_e^2 + p_{\mathrm{F}e}^2}$, $n_e = p_{\mathrm{F}e}^3/3\pi^2$, and similarly for the muons. Electrical neutrality then requires

$$n_p + n_{\Sigma^+} = n_e + n_\mu + n_{\Sigma^-} + n_{\Xi^-} \qquad (16.17)$$

The hyperons and muons will only appear when the baryon chemical potential μ_n is high enough to give them a nonvanishing Fermi momentum.

The total pressure and energy density are expressed in terms of the effective masses and chemical potentials as

$$
\begin{aligned}
P = &\sum_j P_{\mathrm{FG}}(\mu_j^*, m_j^*) + P_{\mathrm{FG}}(\mu_e, m_e) + P_{\mathrm{FG}}(\mu_\mu, m_\mu) \\
&- \tfrac{1}{2} m_\sigma^2 \bar{\sigma}^2 - \tfrac{1}{3} b m_{\mathrm{N}} (g_\sigma \bar{\sigma})^3 - \tfrac{1}{4} c (g_\sigma \bar{\sigma})^4 \\
&+ \tfrac{1}{2} m_\omega^2 \bar{\omega}_0^2 + \tfrac{1}{2} m_\phi^2 \bar{\phi}_0^2 + \tfrac{1}{2} m_\rho^2 (\bar{\rho}_0^3)^2
\end{aligned}
\qquad (16.18)
$$

$$
\begin{aligned}
\epsilon = &\sum_j \epsilon_{\mathrm{FG}}(\mu_j^*, m_j^*) + \epsilon_{\mathrm{FG}}(\mu_e, m_e) + \epsilon_{\mathrm{FG}}(\mu_\mu, m_\mu) \\
&+ \tfrac{1}{2} m_\sigma^2 \bar{\sigma}^2 + \tfrac{1}{3} b m_{\mathrm{N}} (g_\sigma \bar{\sigma})^3 + \tfrac{1}{4} c (g_\sigma \bar{\sigma})^4 \\
&+ \tfrac{1}{2} m_\omega^2 \bar{\omega}_0^2 + \tfrac{1}{2} m_\phi^2 \bar{\phi}_0^2 + \tfrac{1}{2} m_\rho^2 (\bar{\rho}_0^3)^2
\end{aligned}
\qquad (16.19)
$$

where P_{FG} and ϵ_{FG} are the Fermi-gas expressions with the quoted effective masses and chemical potentials

The values of the mean vector fields are determined in a transparent way:

$$m_\omega^2 \bar{\omega}_0 = \sum_j g_{\omega j} n_j$$

$$m_\phi^2 \bar{\phi}_0 = \sum_j g_{\phi j} n_j \qquad (16.20)$$

$$m_\rho^2 \bar{\rho}_0^3 = \sum_j I_{3j} g_{\rho j} n_j$$

The mean value of the scalar field must be determined numerically from the self-consistency condition

$$m_\sigma^2 \bar{\sigma} + b m_N g_{\sigma N}^3 \bar{\sigma}^2 + c g_{\sigma N}^4 \bar{\sigma}^3 = \sum_j g_{\sigma j} n_j^s \qquad (16.21)$$

where n_j^s is the scalar density of the jth baryon.

There are many parameters in $\mathcal{L}_{strong}$. The masses are known. The coupling constants $g_{\omega N}$, $g_{\sigma N}$, b, and c were determined in Chapter 11 on the basis of the nuclear saturation density, binding energy, compressibility, and Landau mass. The ρ–nucleon coupling constant can be determined from the charge symmetry coefficient in the symmetry energy:

$$a_{sym} = \left(\frac{g_{\rho N}}{m_\rho}\right)^2 \frac{p_F^3}{12\pi^2} + \frac{p_F^2}{6 m_L} = 32.5 \text{ MeV} \qquad (16.22)$$

There is considerable uncertainty surrounding the coupling constants in the strange sector. Here we choose $g_{\phi N} = 0$ on the basis that the nucleons have no strange valence quarks while the ϕ meson is composed of $s\bar{s}$. A study of Λ hypernuclei by Rufa *et al.* [2] in the relativistic mean field approximation gives $g_{\sigma\Lambda} = 0.48 g_{\sigma N}$ and $g_{\omega\Lambda} = 0.56 g_{\omega N}$. A study by Keil, Hofmann, and Lenske [3] gives similar numbers, namely, $g_{\sigma\Lambda} = 0.49 g_{\sigma N}$ and $g_{\omega\Lambda} = 0.55 g_{\omega N}$. (For comparison, a study of low-energy nucleon–nucleon and hyperon–nucleon scattering by Maessen, Rijken, and de Swart [4] gives $g_{\sigma\Lambda} = 0.58 g_{\sigma N}$ and $g_{\omega\Lambda} = 0.66 g_{\omega N}$.) These two coupling constants are highly correlated, $g_{\sigma\Lambda}$ being somewhat smaller than $g_{\omega\Lambda}$. The reason is that the binding energy of a Λ hyperon in a nucleus or in nuclear matter depends mainly on the depth of the mean field potential, which is $g_{\omega\Lambda} \bar{\omega}_0 - g_{\sigma\Lambda} \bar{\sigma}_0$. Thus both coupling constants can be increased or decreased together to yield the same mean field potential. For the sake of illustration we shall use the values from Keil *et al.*; based on quark-counting we then estimate that $g_{\sigma\Sigma} = g_{\sigma\Xi} = 0.49 g_{\sigma N}$, $g_{\phi\Lambda} = g_{\omega\Lambda}$, $g_{\omega\Xi} = g_{\omega N}/3$, and $g_{\phi\Xi} = 2 g_{\phi\Lambda}$.

The equation of state for electrically neutral matter, P versus ϵ, is plotted in Figure 16.1. At *low* energy density the pressure of a gas of
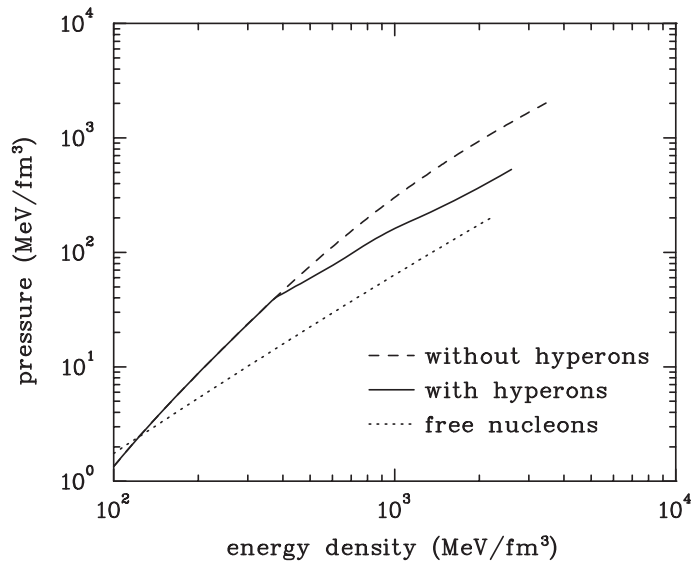
Fig. 16.1.   Equation of state for electrically neutral dense nuclear matter.

noninteracting nucleons (including electrons and muons) is greater than that of nuclear matter that takes into account interactions. The reason is that attractive interactions lower the pressure; in fact, for isospin-symmetric nuclear matter the pressure is zero at the saturation density of nuclear matter. At *high* energy density the situation is reversed; repulsive interactions involving vector mesons cause an increase in the pressure. When hyperons are included the pressure is reduced and the equation of state is said to be softened, on account of energy having been put into hyperon masses rather than into the kinetic energy of nucleons.

The star mass as a function of central energy density, for each of the three model equations of state, is plotted in Figure 16.2. These are obtained as solutions to the Tolman–Oppenheimer–Volkoff equation. The star mass at first increases with central density, reaches a maximum, and then decreases. The maximum mass represents the limit of stability. A star cannot be supported against gravitational collapse to a black hole by going beyond that limit. As can be seen by comparing Figures 16.1 and 16.2, a stiffer equation of state can support a higher maximum mass. A large number of neutron star masses have been measured in binary star systems. The most accurately measured ones tend to fall in the range between 1.4 and 1.5 solar masses. This proves observationally that nuclear interactions are crucial in supporting a neutron star from gravitational collapse; a gas of free neutrons, protons, electrons, and muons can only produce a star with maximum mass less than 0.7 solar mass.
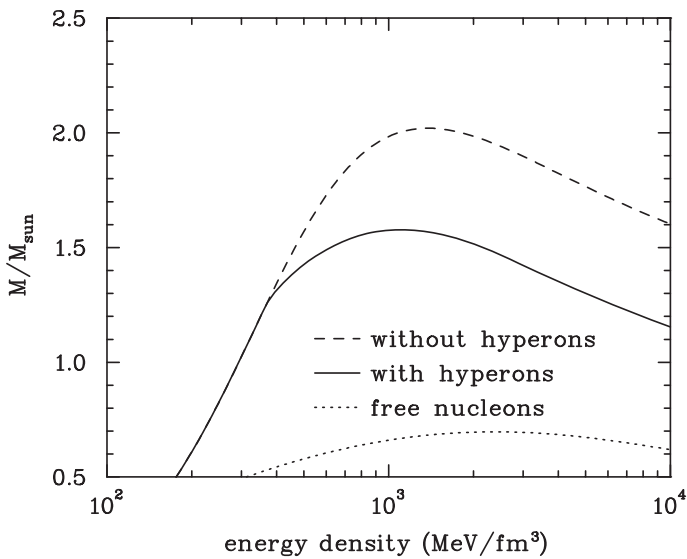
Fig. 16.2. Star mass as a function of central energy density for the three equations of state represented in Figure 16.1.

The chemical abundances of the baryons are very interesting. These are shown in Figure 16.3 for the model equation of state that includes hyperons. At low baryon density the matter is dominated by neutrons. Neutron decay is Pauli-blocked by a small admixture of protons and electrons. As the density goes up it is advantageous for more neutrons to be converted to protons and electrons. Eventually it becomes favorable for nucleons to be converted into hyperons. This is a general feature. However, the order of appearance of hyperons with density and their relative abundances depend sensitively on the numerical values of the coupling constants. Increasing the coupling to the scalar field decreases the effective mass, and decreasing the coupling to the vector fields increases the effective chemical potential, both of which work to favor the appearance of a given hyperon. Note, however, that the maximum-mass star only probes the equation of state up to an energy density of about 1 GeV fm^{-3} and a baryon density of about $0.9 \text{ fm}^{-3} \approx 6n_0$, where n_0 is the nuclear saturation density.

Whether the central density in the most massive neutron stars is great enough to support a core of quark matter has been a topic of much study and debate over the last three decades; if so, the core may be a color superconductor, as described in Section 8.9. Unfortunately, it is very difficult to probe the deep interior of a cold neutron star. A neutron star is born in a supernova, however, and therefore has an initial temperature
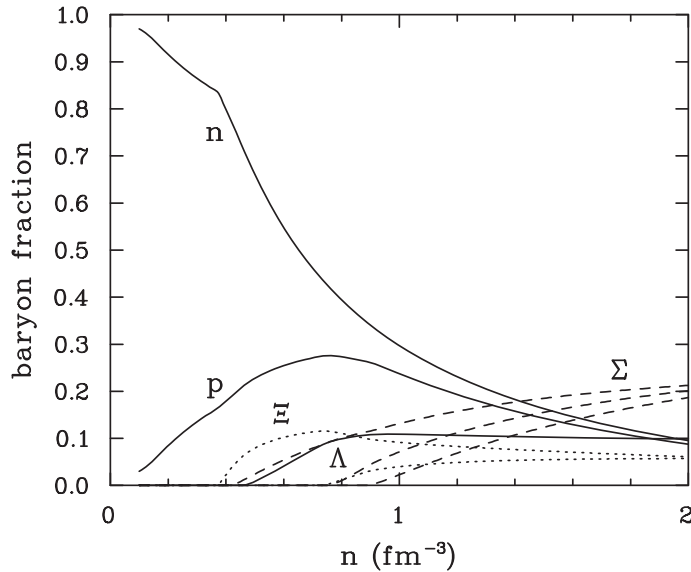
Fig. 16.3. Baryon chemical composition for the equation of state that includes hyperons. Note that the cusps correspond to particle production thresholds.

that may be as high as 40 MeV. The interior of the star cools by several mechanisms, including neutrino production. This is a topic to which we turn our attention now.

16.3 Neutrino emissivity

As mentioned in the previous section, neutron stars are born with a significant amount of thermal energy. A great deal of this is lost by neutrino emission. The microscopic processes are quite varied and complicated. The environments for these processes are usually separated into the outer crust and the inner core; the inner core may be nonsuperfluid or it may be superfluid and magnetized.

Two of the most important reactions in the crust are pair annihilation, $e^+e^- \to \nu\bar{\nu}$, and plasma decay, $\gamma \to \nu\bar{\nu}$. Pair annihilation is quite straightforward, but it was not until 1993 that a fully relativistic treatment of plasma decay (actually the decay of collective excitations of the plasma) was carried out, by Braaten and Segel [5]. One of the most important reactions in the crust is the direct Urca process, $n \to pe^-\bar{\nu}_e$, and the related reaction $pe^- \to n\nu_e$. (The process was named after a casino in Rio de Janeiro by Gamow and Schoenberg [6] who likened thermal energy to money and neutrinos to the casino that takes it away.) There is also a modified Urca process, in which a spectator nucleon N facilitates the

process, namely, $nN \to pNe^-\bar{\nu}_e$ and $pNe^- \to nN\nu_e$. The nucleon N, or the neutron or proton for that matter, may be replaced by a hyperon, depending on the chemical conditions in the core. Then there is neutrino cooling by more exotic processes, such as pion condensation, kaon condensation, the Urca process for quarks, or color superconductivity. We shall consider some of these processes in this section. For a comprehensive survey the reader should consult the review by Yakovlev *et al.* [7].

16.3.1 Pair annihilation

When the temperature of the crust or the core reaches 100 keV or so, which is a significant fraction of the electron mass, there will be a significant number of electrons and positrons which can annihilate into neutrino–antineutrino pairs. The rate (number of reactions per unit time per unit volume) can be calculated directly from the cross section:

$$dR = \sigma(e^+e^- \to \nu_l\bar{\nu}_l)v_{\text{rel}} \left(2\frac{d^3p_-}{(2\pi)^3}N_{\text{F}}^-(p_-) \right) \left(2\frac{d^3p_+}{(2\pi)^3}N_{\text{F}}^+(p_+) \right) \quad (16.23)$$

Here the subscript l specifies the neutrino flavor and $v_{\text{rel}} = \sqrt{(p_+ \cdot p_-)^2 - m_e^4}/E_+E_-$; the quantities in large parentheses represent the thermal phase space for electrons and positrons, including the spin factor 2 (the Fermi–Dirac occupation numbers are the same as in (5.57)). This expression assumes that neutrinos escape so that there is no Pauli-blocking in the final state. Note that the cross section is proportional to the imaginary part of the forward scattering amplitude and to the square of the invariant amplitude, as discussed in Section 12.2. The same expression can be derived from the finite-temperature field theory rules using the standard model Lagrangian. For the present situation, where the temperature and chemical potential are smaller than the electroweak scale of 100 GeV, we might as well use the cross section as calculated in many texts on the standard model.

The neutrino emissivity Q is the energy radiated into neutrinos per unit time per unit volume. This involves multiplication of dR by the total energy $E_+ + E_-$ and integration over all phase space:

$$\begin{aligned}
Q_{\text{pair}} = \frac{G_{\text{F}}^2}{3\pi} \int &\left(\frac{d^3p_-}{(2\pi)^3}N_{\text{F}}^-(p_-) \right) \left(\frac{d^3p_+}{(2\pi)^3}N_{\text{F}}^+(p_+) \right) (E_+ + E_-) \\
&\times \left\{ C_+^2 \left[m_e^4 + 3m_e^2(p_- \cdot p_+) + 2(p_- \cdot p_+)^2 \right] \right. \\
&\left. + 3m_e^2 C_-^2 \left[m_e^2 + (p_- \cdot p_+) \right] \right\}
\end{aligned} \quad (16.24)$$

The Fermi constant is denoted by G_{F}. The quantities $C_\pm^2 = \sum_l(C_{Vl}^2 \pm C_{Al}^2)$ are sums over neutrino flavors of the vector and axial-vector

constants. Electron neutrinos can be produced via charged or neutral current interactions, involving W and Z vector bosons, respectively, while muon and tau neutrinos can only be produced via neutral current interactions. Thus $C_{Ve} = 2\sin^2\theta_{\mathrm{W}} + 1/2$, $C_{Ae} = 1/2$, $C_{V\mu} = C_{V\tau} = 2\sin^2\theta_{\mathrm{W}} - 1/2$, $C_{A\mu} = C_{A\tau} = -1/2$, with $\sin^2\theta_{\mathrm{W}} \approx 0.23$. The six-dimensional integral for Q_{pair} can be reduced to products of one-dimensional integrals. The latter cannot be found in closed form in general, but they can be evaluated numerically; simple parametrizations for them also exist (see [7]).

A particularly simple limit, although not the most relevant for the majority of periods of neutron star cooling, is the nondegenerate ($N_{\mathrm{F}} \ll 1$) ultrarelativistic ($T \gg m_e$) limit;

$$Q_{\mathrm{pair}} \to \frac{7\zeta(5)}{12\pi} C_+^2 G_{\mathrm{F}}^2 T^9 \qquad (16.25)$$

This illustrates how rapidly the cooling rate increases with temperature. In this limit, a ten-fold increase in T results in a billion-fold increase in the emissivity!

16.3.2 Plasma decay

We saw in Chapter 6 that the photon propagator at finite temperature has singularities corresponding to the propagation of transverse and longitudinal modes. Both modes have a finite energy at zero momentum. As a consequence, they will decay into a neutrino–antineutrino pair. This occurs via the coupling of the photon to a (virtual) e^+e^- pair, which then annihilates into neutrinos. The general expression for the emissivity is

$$Q_{\mathrm{plasma}} = \int \frac{d^3k}{(2\pi)^3} \left[2N_{\mathrm{B}}(\omega_{\mathrm{T}})\omega_{\mathrm{T}}\Gamma_{\mathrm{T}}(\omega_{\mathrm{T}}) + N_{\mathrm{B}}(\omega_{\mathrm{L}})\omega_{\mathrm{L}}\Gamma_{\mathrm{L}}(\omega_{\mathrm{L}}) \right] \qquad (16.26)$$

The N_{B} are the Bose-Einstein distributions, ω_{T} and ω_{L} are the energies of the transverse and longitudinal modes with momentum k, and Γ_{T} and Γ_{L} are the decay rates into a $\nu\bar{\nu}$ pair.

The complete one-loop analysis of the plasma decay rates at arbitrary temperature and chemical potential was carried out by Braaten and Segel [5]. The rates are expressed in terms of the photon longitudinal and transverse self-energies, F and G, and the residues of their poles, Z_{L} and Z_{T}. Specifically, $Z_{\mathrm{L}}^{-1}(k_0, \mathbf{k}) = 1 - \partial F(k_0, \mathbf{k})/\partial k_0^2$ and

$Z_{\mathrm{T}}^{-1}(k_0, \mathbf{k}) = 1 - \partial G(k_0, \mathbf{k})/\partial k_0^2$. We have

$$\Gamma_{\mathrm{T}}(k_0, \mathbf{k}) = \frac{G_{\mathrm{F}}^2}{48\pi^2\alpha} Z_{\mathrm{T}}(k_0, \mathbf{k}) \frac{k^2}{k_0} \left[C_V^2 G^2(k_0, \mathbf{k}) + C_A^2 \Pi_A^2(k_0, \mathbf{k}) \right]$$

$$\Gamma_{\mathrm{L}}(k_0, \mathbf{k}) = \frac{G_{\mathrm{F}}^2}{48\pi^2\alpha} Z_{\mathrm{L}}(k_0, \mathbf{k}) \frac{k^2}{k_0} C_V^2 F^2(k_0, \mathbf{k})$$

$$(16.27)$$

The transverse rate also involves a new axial self-energy Π_A. To leading order in α it is given by

$$\Pi_A(k) = e^2 \frac{k^2}{|\mathbf{k}|} \int \frac{d^3p}{(2\pi)^3 E} \left[N_{\mathrm{F}}^-(E) - N_{\mathrm{F}}^+(E) \right] \frac{k_0(p \cdot k) - Ek^2}{(p \cdot k)^2 - (k^2)^2/4} \quad (16.28)$$

where $E = \sqrt{\mathbf{p}^2 + m_e^2}$. To first order in α, the term $(k^2)^2/4$ in the denominator can be set to zero; it corresponds to an imaginary part arising from the production of electron–positron pairs. This is unphysical since it does not take into account the dispersion relation of electrons to the same order in α. The resulting expression for Π_A can be expressed as a one-dimensional integral that in general must be done numerically. When used to calculate the emissivity, all functions above are evaluated using the appropriate dispersion relation, either $k_0 = \omega_{\mathrm{L}}(\mathbf{k})$ or $k_0 = \omega_{\mathrm{T}}(\mathbf{k})$.

For neutron star cooling it is numerically efficient to have simple, accurate, analytic formulas for the emissivity. Nice formulas were derived by Braaten and Segel with this in mind. The following expressions were shown to be correct in the classical, degenerate, and relativistic limits for all momenta and correct at small momenta for all temperatures and densities; they were interpolated to an accuracy of order α in between these limits (in what follows $k = |\mathbf{k}|$):

$$\omega_{\mathrm{T}}^2 = k^2 + \omega_{\mathrm{P}}^2 \frac{3\omega_{\mathrm{T}}^2}{2v_*^2 k^2} \left[1 - \frac{\omega_{\mathrm{T}}^2 - v_*^2 k^2}{2v_* k \omega_{\mathrm{T}}} \ln\left(\frac{\omega_{\mathrm{T}} + v_* k}{\omega_{\mathrm{T}} - v_* k} \right) \right] \qquad 0 \leq k < \infty$$

$$(16.29)$$

$$\omega_{\mathrm{L}}^2 = \omega_{\mathrm{P}}^2 \frac{3\omega_{\mathrm{L}}^2}{v_*^2 k^2} \left[\frac{\omega_{\mathrm{L}}}{2v_* k} \ln\left(\frac{\omega_{\mathrm{T}} + v_* k}{\omega_{\mathrm{T}} - v_* k} \right) - 1 \right] \qquad 0 \leq k < k_{\max} \quad (16.30)$$

$$k_{\max} = \sqrt{\frac{3}{v_*^2} \left[\frac{1}{2v_*} \ln\left(\frac{1 + v_*}{1 - v_*} \right) - 1 \right]} \, \omega_{\mathrm{P}} \qquad (16.31)$$

$$v_*^2 \omega_{\mathrm{P}}^2 = \frac{4\alpha}{3\pi} \int_0^\infty \frac{dp\, p^2}{E} \left[5\left(\frac{p}{E} \right)^2 - 3\left(\frac{p}{E} \right)^4 \right] N_{\mathrm{F}}(E) \qquad (16.32)$$

In these expressions ω_{P} is the plasma frequency, defined in Chapter 6. The variable v_* lies between 0 and 1. Since we start with two independent

variables, T and μ, it is quite natural that the two independent variables ω_P and v_* appear in the result. The longitudinal and transverse energies must still be solved self-consistently from this set of equations.

When evaluated with the dispersion relations calculated above, the self-energies and residues are approximated to the same accuracy, as follows:

$$F = \omega_L^2 - k^2 \tag{16.33}$$

$$G = \omega_T^2 - k^2 \tag{16.34}$$

$$Z_T = \frac{2\omega_T^2(\omega_T^2 - v_*^2 k^2)}{3\omega_P^2\omega_T^2 + (\omega_T^2 + k^2)(\omega_T^2 - v_*^2 k^2) - 2\omega_T^2(\omega_T^2 - k^2)} \tag{16.35}$$

$$Z_L = \frac{2\omega_L^2(\omega_L^2 - v_*^2 k^2)}{(\omega_L^2 - k^2)[3\omega_P^2 - (\omega_L^2 - v_*^2 k^2)]} \tag{16.36}$$

$$\Pi_A = \omega_A k \frac{(\omega_T^2 - k^2)[3\omega_P^2 - 2(\omega_T^2 - k^2)]}{\omega_P^2(\omega_T^2 - v_*^2 k^2)} \tag{16.37}$$

One new frequency appears, which is

$$\omega_A = \frac{2\alpha}{3\pi} \int_0^\infty dp \left[3\left(\frac{p}{E}\right)^2 - 2\left(\frac{p}{E}\right)^4 \right] [N_F^-(E) - N_F^+(E)] \tag{16.38}$$

To calculate the emissivity, first the two dispersion relations must be solved numerically and inserted into the functions appearing in the integrand, and then the one-dimensional integral must be evaluated numerically. However, several limits can be evaluated analytically. Consider the high-temperature limit defined by $T \gg \omega_P$. It can be shown that the contribution of the longitudinal part is smaller than that of the transverse part by a factor of order ω_P^2/T^2, and the axial part is smaller by a factor of order ω_A^2/T^2. The transverse part can be evaluated by setting the factor $\omega_T^2 - k^2$ equal to $m_P^2 = G(k_0 = |\mathbf{k}|)$ (see Section 6.7) because the integral is dominated by $k \gg \omega_T$, and otherwise setting $\omega_T = k$. The emissivity is then given by

$$Q_{\text{plasma}} \rightarrow \frac{G_F^2}{24\pi^4\alpha} C_V^2 \zeta(3) m_P^6 T^3 \tag{16.39}$$

In the limit $T \gg |\mu_e|$ and $T \gg m_e$, $m_P^2 \propto \alpha T^2$. Then the emissivity goes as $\alpha^2 G_F^2 T^9$. The powers of the couplings follow from the lowest-order diagrams needed to make the process go, and the power of the temperature follows from dimensional analysis.

16.3.3 Direct Urca process for quarks

The analog of the direct Urca process for quarks is $d \rightarrow u + e^- + \bar{\nu}_e$ and $u + e^- \rightarrow d + \nu_e$. In beta equilibrium the chemical potentials are related

by

$$\mu_d = \mu_s = \mu_u + \mu_e \tag{16.40}$$

If the particles are assumed to be massless, electrical neutrality is achieved without any electrons:

$$\begin{aligned} n_u = n_d = n_s = n \\ n_e = 0 \end{aligned} \tag{16.41}$$

where n is the baryon density. At low temperatures the quark Urca process can only occur when all particles are near their Fermi surface; hence, there is very little phase space for the reactions to occur. In particular, if all particles are massless then energy and momentum conservation requires the up quark, down quark, and electron momenta all to be collinear. Giving the d quark a slightly greater mass than the u quark, say 7 MeV versus 5 MeV, does allow the decay to proceed, but very slowly. Iwamoto [8] showed that interactions among the quarks change the situation dramatically.

From Chapter 8 we know that the relation between the Fermi momentum, defined via the density, and the chemical potential is

$$\mu_q = \left(1 + \frac{2}{3\pi}\alpha_s\right) p_{\mathrm{F}q} \tag{16.42}$$

for quark flavors $q = u, d$. For relativistic electrons,

$$\mu_e \approx p_{\mathrm{F}e} \tag{16.43}$$

Therefore $p_{\mathrm{F}d} - p_{\mathrm{F}u} - p_{\mathrm{F}e} \approx -(2/3\pi)\alpha_s p_{\mathrm{F}e} < 0$. This opens up the phase space for the reactions and allows them to occur at a much higher rate. Knowing the decay rate for the down quark, and the cross section for the flavor-changing reaction, both of which could easily be calculated within the standard model, Iwamoto found their sum to be

$$Q_{\mathrm{quark\,Urca}} = \frac{457}{630} G_{\mathrm{F}}^2 \alpha_s \cos^2\theta_{\mathrm{C}} \, p_{\mathrm{F}d} \, p_{\mathrm{F}u} \, p_{\mathrm{F}e} \, T^6 \tag{16.44}$$

where θ_{C} is the Cabibbo angle with $\cos^2\theta_{\mathrm{C}} \approx 0.948$. The electron Fermi momentum would be zero if the strange quark mass were zero, but it is not. For the temperatures of interest, say 5 to 50 MeV, $p_{\mathrm{F}e}$ is comparable to T, while $p_{\mathrm{F}d}$ and $p_{\mathrm{F}u}$ are definitely larger than T. The QCD coupling is in the range of 0.1 to 1.0. Therefore the quark Urca process provides quite a large emissivity.

There is also the direct Urca process in which the strange quark replaces the down quark. The current-quark value of the strange quark mass at the scales of relevance is around 105 to 150 MeV. This suppresses the

reaction $u + e^- \to s + \nu_e$ but enhances the decay $s \to u + e^- + \bar{\nu}_e$. However, the latter is suppressed by the factor $\sin^2 \theta_C \approx 0.052$ because it is a strangeness-changing process. Overall one finds that the direct Urca process with the strange quark is smaller than with the down quark.

If the electron Fermi momentum becomes too small then the modified quark Urca process $d + q \to u + q + e^- + \bar{\nu}_e$ and $u + q + e^- \to d + q + \nu_e$ dominates. This was calculated by Burrows [9].

16.4 Cosmological QCD phase transition

The main interest in a cosmological quark–gluon to hadron phase transition arises from its potential to influence the big bang nucleosynthesis. Whether QCD with its known set of parameters undergoes a first-order transition or something smoother is still not completely settled. Assuming that there is a first-order phase transition one needs nucleation theory to understand how the transition proceeds; this topic was discussed in Chapter 13. In this section we first discuss how it can be that nucleosynthesis is affected by a QCD phase transition, and then we analyze the dynamics of a first-order phase transition during the expanding early universe.

16.4.1 Inhomogeneous big bang nucleosynthesis

A cosmological first-order phase transition at $T \sim 160 - 180$ MeV could leave spatial inhomogeneities in the baryon-to-entropy ratio and in the ratio of protons and neutrons. If these inhomogeneities survive to $T \sim 0.1$–1 MeV then they could influence nucleosynthesis. This was first pointed out and analyzed by Witten [10], by Applegate, Hogan, and Scherrer [11], and by Alcock, Fuller, and Mathews [12]. In thermal and chemical equilibrium one might expect that the baryon density in the quark–gluon phase is higher than in the hadron phase. This is called the baryon density contrast. Assuming a critical temperature of $160 < T_c < 180$ MeV, Kapusta and Olive [13] computed this baryon density contrast to be 1.5 to 2.5 when hadronic interactions were neglected and 5 to 7 when they were included. One would expect that the last regions of space to undergo the phase conversion would contain more baryons per unit volume than the first regions to phase-convert because of the lack of time for baryons to diffuse. After phase completion the neutrons will diffuse more rapidly than protons because they are electrically neutral and therefore do not Coulomb-scatter on electrons. This leads to isospin inhomogeneities, at least temporarily.

A detailed calculation of inhomogeneous nucleosynthesis with a comparison to the observed abundances of the light elements was performed
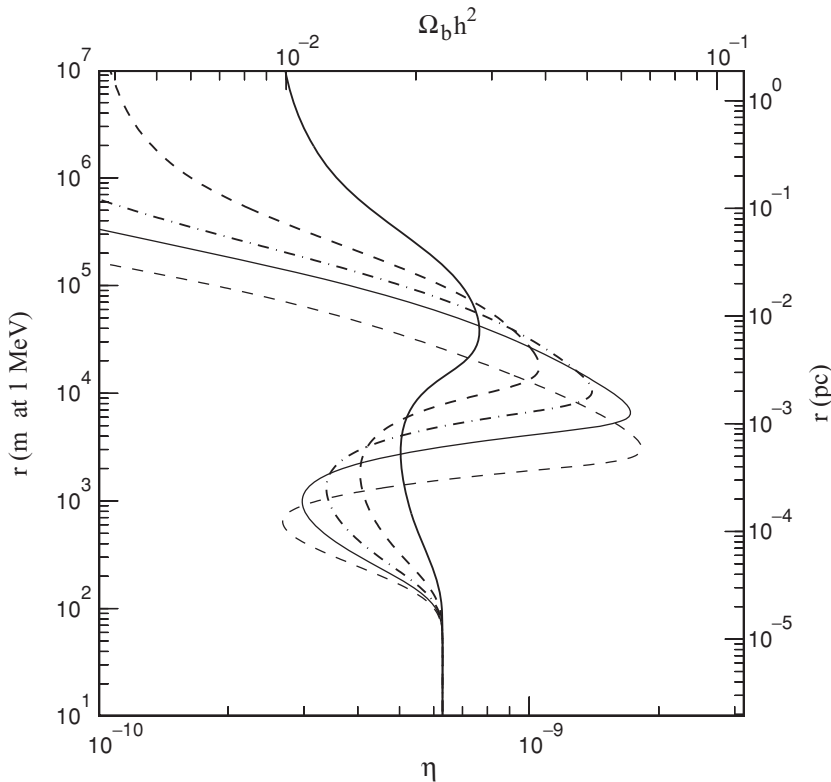
Fig. 16.4. Conservative upper limit to the baryon-to-photon ratio η from the ^{4}He abundance $Y_p \leq 0.248$ and the deuterium abundance $D/H \geq 1.5 \times 10^{-5}$. The three thicker curves are for volume fractions covered by the high-density regions of $1/(2\sqrt{2})$ (solid), $1/8$ (broken), and $1/(16\sqrt{2})$ (broken and dotted). The two thinner curves are for volume fractions $1/64$ (solid) and $1/256$ (broken). From [15].

by Kurki-Suonio *et al.* [14]. They considered baryon density contrasts ranging from 1 to 100 and matter-fractions in the high-density regions ranging from $1/64$ to $1/4$. The average separation of the high-density regions l was left as a free parameter, as was the average baryon-to-photon ratio of the universe. The differential diffusion of protons and neutrons was accounted for and then a standard nucleosynthesis code was run. By fitting the observed abundances of ^{4}He, D, ^{3}He, and ^{7}Li they concluded that the baryon-to-photon ratio must lie between 2×10^{-10} and 7×10^{-10} (or 20×10^{-10} if certain constraints on ^{7}Li were relaxed). They also concluded that $l < 150$ m at the time of nucleosynthesis, whereas at the completion of the QCD phase transition this upper limit would have been only about 1 m. A quantitative theoretical estimate of the latter scale is the purpose of the next subsection.

Recently the inhomogeneous nucleosynthesis calculation was redone, with technical improvements and updated estimates of the cosmic abundances of the relevant light elements, by Kainulainen, Kurki-Suonio, and Sihvola [15]. Their results are shown in Figure 16.4. The high-density matter was distributed in spheres. The inhomogeneities are ineffective in influencing nucleosynthesis unless the high-density regions are separated by more than about 150 m at $T = 1$ MeV.

16.4.2 Dynamics of the phase transition

The nucleation rate for a system of particles or fields that has negligible baryon number compared with the entropy was derived in Section 13.4. Here we mention only the essential details. The change in free energy due to the appearance of a bubble of hadronic matter in quark–gluon plasma is

$$\Delta F = \frac{4\pi}{3} r^3 \left[P_q(T) - P_h(T) \right] + 4\pi r^2 \sigma \tag{16.45}$$

where r is the radius. The critical-sized bubble has radius

$$r_* = \frac{2\sigma}{P_h(T) - P_q(T)} \tag{16.46}$$

which leads to

$$\Delta F_* = \frac{4\pi}{3} \sigma r_*^2 \tag{16.47}$$

The nucleation rate is

$$I = \frac{4}{\pi} \left(\frac{\sigma}{3T} \right)^{3/2} \frac{\sigma(3\zeta_q + 4\eta_q) r_*}{3(\Delta w)^2 \xi_q^4} e^{-\Delta F_*/T} \tag{16.48}$$

It is proportional to the shear viscosity η_q and the bulk viscosity ζ_q in the quark–gluon plasma and is inversely proportional to the square of the enthalpy ($w = \epsilon + P$) difference between the two phases.

For numerical purposes we use a simple bag-model-type equation of state with

$$P_q = (45.5 + 14.25) \frac{\pi^2}{90} T^4 - B$$

$$P_h = (5.5 + 14.25) \frac{\pi^2}{90} T^4 \tag{16.49}$$

The constant 45.5 approximates the effective number of degrees of freedom arising from massless gluons and up and down quarks and a strange quark mass comparable with the temperature. The constant 5.5 approximates the hadronic equation of state near T_c arising from a multitude of massive

hadrons. The constant 14.25 arises from photons, neutrinos, electrons, and muons common to both phases. The bag constant B is chosen to give $T_c = 160$ MeV. For definiteness we take $\sigma = 50$ MeV/fm^2, $\xi_q = 0.7$ fm, and $\eta_q = 18T^3$ (see Section 9.6 and Baym *et al.* [16]).

Given the nucleation rate one would like to know the (volume) fraction of space $h(t)$ that has been converted from the quark–gluon plasma to hadronic gas at proper time t in the early universe. This requires kinetic equations that use the nucleation rate I as an input. Here we use a rate equation first proposed by Csernai and Kapusta [17]. The nucleation rate I is the probability of forming a bubble of critical size per unit time per unit volume. If the system cools to T_c at time t_c then at some later time t the fraction of space that has been converted to the hadronic phase is

$$h(t) = \int_{t_c}^{t} dt' \ I(T(t'))[1 - h(t')]V(t', t) \tag{16.50}$$

Here $V(t', t)$ is the volume of a hadronic bubble at time t that was nucleated at an earlier time t'; this takes into account bubble growth. The factor $1 - h(t')$ takes into account the fact that new bubbles can only be nucleated in the fraction of space not already occupied by the hadronic gas. This conservative approach neglects any spatial variation in the temperature. However, it does allow for completion of the transition without violating any of the fundamental laws of thermodynamics.

Next we need a dynamical equation that couples the time evolution of the temperature to the fraction of space converted to the hadronic phase. We use Einstein's equations as applied to the early universe, neglecting curvature. The evolution of the energy density is

$$\frac{d\epsilon}{dR} = -\frac{3w}{R} \tag{16.51}$$

where R is the scale factor at time t. This assumes kinetic but not phase equilibrium and is basically a statement of energy conservation. We express the energy density as

$$\epsilon = h\epsilon_h(T) + (1 - h)\epsilon_q(T) \tag{16.52}$$

where ϵ_h and ϵ_q are the energy densities in the two phases at the temperature T. There is a similar equation for the enthalpy w. The time dependence of the scale factor is determined by the equation of motion

$$\frac{1}{R}\frac{dR}{dt} = \sqrt{\frac{8\pi G\epsilon}{3}} \tag{16.53}$$

This expression can be used to relate the time to the scale factor using the normalization $R(t_c) = 1$.
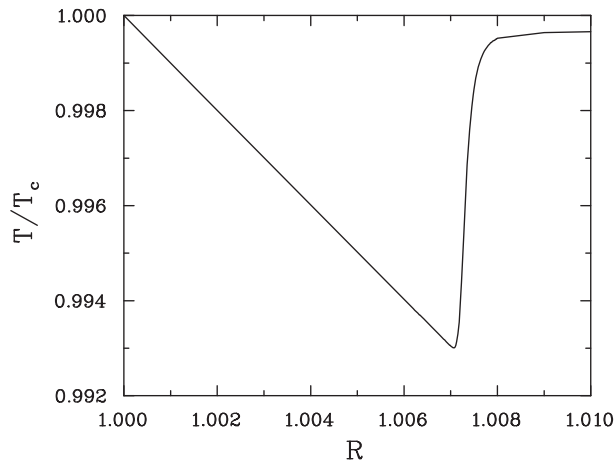
Fig. 16.5.   Temperature as a function of scale factor.

We also need to know how fast a bubble expands once it is created. This is a subtle issue since by definition a critical-sized bubble is metastable and will not grow without a perturbation. After applying a perturbation, a critical-sized bubble begins to grow. As the radius increases the surface curvature decreases, and an asymptotic interfacial velocity is approached. The asymptotic radial-growth velocity will be referred to as $v(T)$. The expected qualitative behavior of $v(T)$ is that the closer T is to T_c the more slowly the bubbles grow. At T_c there is no motivation for bubbles to grow at all since one phase is as good as the other. The bubble-growth velocity was studied by Miller and Pantano [18]. Their hydrodynamical results may be parametrized by the simple formula

$$v\gamma = 3\left(1 - \frac{T}{T_c}\right)^{3/2} \tag{16.54}$$

which indeed has the expected behavior. A simple illustrative model for bubble growth is then

$$V(t', t) = \frac{4\pi}{3}\left[r_*(T(t')) + \int_{t'}^{t} dt'' v(T(t''))\right]^3 \tag{16.55}$$

This expression can also be written in terms of R, R', R'' instead of t, t', t''.

We now have a complete set of coupled integro-differential equations, which must be solved numerically. These equation take into account bubble nucleation and growth, energy conservation, and Einstein's equations. They make no assumption about entropy conservation.

Figure 16.5 shows the temperature as a function of the scale factor. For practical purposes, nucleation begins near the bottom of the cooling
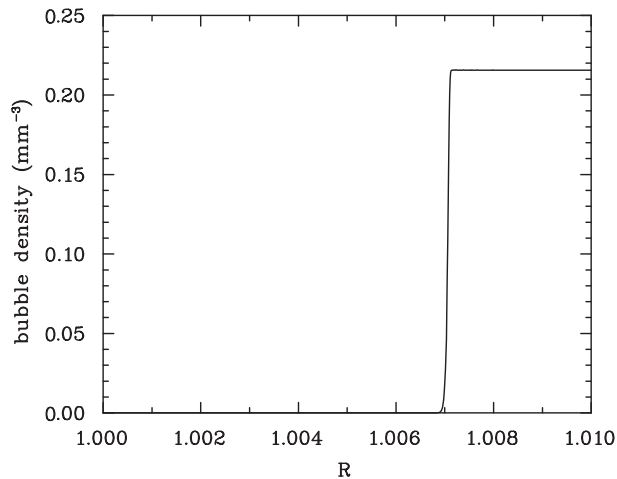
Fig. 16.6.   Average bubble density as a function of scale factor.

line. Thereafter, the nucleation and growth of bubbles release latent heat that causes the temperature to rise. The increasing temperature shuts off nucleation, and the phase transition continues owing to the growth of already nucleated bubbles. The temperature can never quite reach T_c; if it did, bubble growth would cease and the transition would never complete. This is a result of the equations of motion and is not an imposition.

Figure 16.6 shows the average bubble density

$$n(R(t)) = \int_{t_c}^{t} dt'\, I(T(t'))[1 - h(t')] \tag{16.56}$$

as a function of the scale factor. The bubble density rises rapidly just before R reaches 1.007 and reaches its asymptotic value just after 1.007.

Figure 16.7 shows the nucleation rate as a function of scale factor. The rate has a very sharp maximum between 1.0070 and 1.0071. The turn-on and turn-off of the nucleation rate corresponds precisely with the fall and rise of the temperature shown in Figure 16.5.

Figure 16.8 shows the fraction of space h that has made the conversion to the hadronic phase. When $h = 1$ the transition is complete and the temperature will begin to fall again. This occurs when $R \approx 1.4464$, to be compared with the value one would obtain from an ideal Maxwell construction, $R_{\text{Maxwell}} = (239/79)^{1/3} = 1.446\,30. \ . \ . \ .$ In fact the whole curve $h(R)$ is very close to the ideal Maxwell construction, apart from its
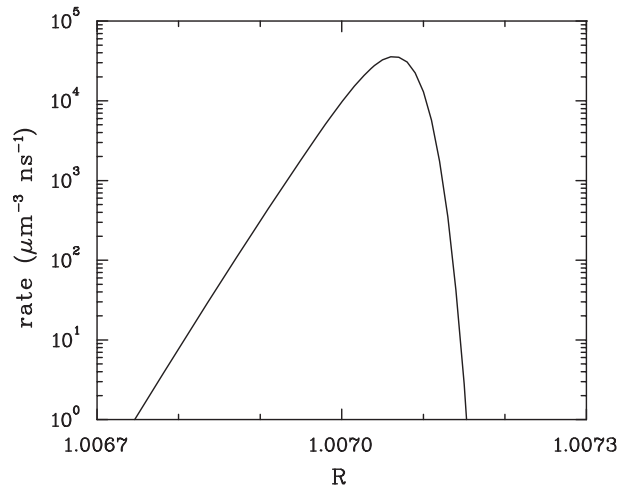
Fig. 16.7.   Nucleation rate as a function of scale factor.
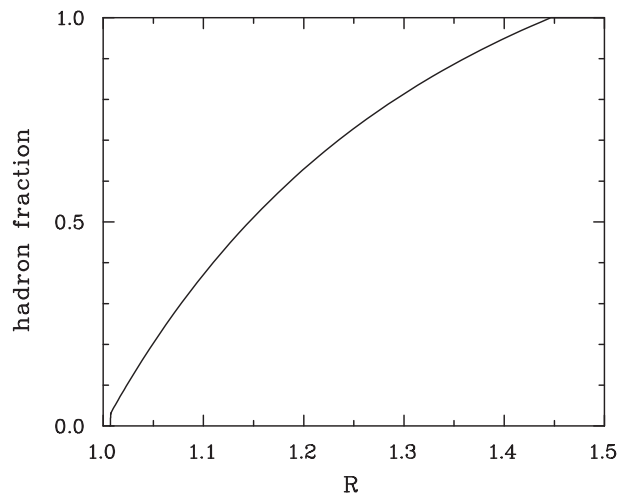
Fig. 16.8.   Volume fraction of space h occupied by the hadronic phase as a function of scale factor.

delayed start, apparent in the figure. The interested reader could work out the Maxwell formula from the equations given here.

Figure 16.9 shows the average bubble radius $\bar{r}$ as a function of scale factor, obtained from

$$\frac{4\pi}{3}\bar{r}^3 n = h \tag{16.57}$$
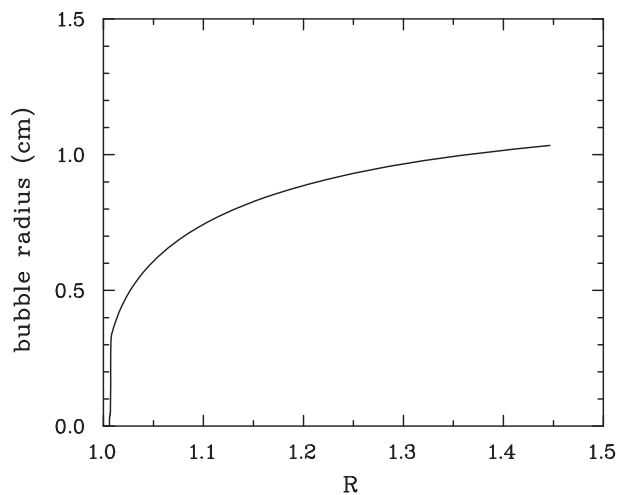
Fig. 16.9. Average bubble radius as a function of scale factor.

It grows with time and with the scale factor, of course. At the end of the phase transition it is of order 1 cm. This is also the order of magnitude of the distance between the final quark–gluon plasma regions. Unfortunately, it is two orders of magnitude too small to affect nucleosynthesis. This result is rather robust against reasonable variations in any of the input parameters.

Nucleosynthesis is affected by remnant inhomogeneities in the baryon-to-entropy ratio and in isospin if the high-baryon-density regions immediately following a QCD phase transition are separated by at least 1 m. A set of dynamical equations can be written and solved for the evolution of the universe through such a phase transition all the way to completion. The evolution of the temperature and hadronic volume fraction as functions of time and scale factor are hardly different from the results of an idealized Maxwell construction. The information not available in the latter construction is the length scale of the inhomogeneities, that is, bubble sizes and so on. The characteristic distance between the last regions of quark–gluon plasma seem to be of order 1 cm, too small to affect nucleosynthesis. However, qualifications and improvements can be made. For example, when the fraction of space occupied by bubbles exceeds about 50%, interactions among the bubbles probably cannot be neglected. It is unlikely, though, that further improvements in the dynamics would qualitatively change the current picture of the transition. Indeed, crude estimates of the effects of bubble fusion on the dynamics of the QCD transition in heavy ion collisions indicate that the transition completes only a little faster, and that the average bubble size is greater (Csernai *et al.* [19]). At least this is in the right direction to be interesting.

16.5 Electroweak phase transition and baryogenesis

The standard model conserves baryon and lepton number at the classical level but not at the quantum level. This violation is always a possibility when the current is associated with a global symmetry rather than with a local gauge symmetry. Electric charge, for example, is conserved at both the classical and quantum levels. This phenomenon is called the Adler–Bell–Jackiw anomaly (Bell and Jackiw [20]; Adler [21]). In the standard model the divergence of the baryon current is

$$\partial_\mu J_B^\mu = \frac{N_{\text{fam}}}{64\pi^2}\epsilon^{\mu\nu\rho\sigma}\left(g^2 f_{\mu\nu}^a f_{\rho\sigma}^a + g'^2 g_{\mu\nu}g_{\rho\sigma}\right) \qquad (16.58)$$

Entering on the right-hand side are the field strength tensors for the SU(2) and U(1) gauge fields, in the same notation as in Chapter 15. There is a factor N_{fam} on the right-hand side equal to the number of quark families (the standard model has three). The divergence of the lepton current is exactly the same, so that if the numbers of families of quarks and leptons are the same, as in the standard model, the baryon number minus the lepton number, $B - L$, is conserved. Of course, baryon and lepton number will change only if the field configurations are such that the right-hand side does not vanish.

Gerard 't Hooft [22] showed that, indeed, the conservation of baryon number is violated by the instanton of the weak SU(2) group. (For instantons in QCD see Chapter 8.) The rate for baryon number violation is proportional to the factor $\exp(-16\pi^2/g^2) \approx 10^{-170}$. The probability of observing this effect is exceedingly small with any reasonable estimate of the prefactor. The proton lifetime, for example, has been estimated to be many orders of magnitude larger than the age of the universe. It would seem that this effect is merely a curiosity of quantum field theory.

However, Kuzmin, Rubakov, and Shaposhnikov [23] showed that this is not the case at high temperatures. The reason that baryon number can be violated at zero or low temperatures is that the weak instanton involves tunneling between inequivalent vacua with different baryon numbers. This tunneling is exponentially suppressed by the aforementioned factor. At high temperatures the transition can occur because of thermal fluctuations, and if the temperature is high enough the corresponding Boltzmann factor may not be nearly as small as the tunneling probability. Specifically, they calculated the free energy of a static classical field configuration involving the SU(2) gauge field and the Higgs field. The Boltzmann factor for the baryon-number-violating process is

$$\exp\left(\frac{-F_{\text{sphaleron}}}{T}\right) = \exp\left[\int_0^\beta d\tau \int d^3x \,\mathcal{L}_{\text{eff}}(A_i^a(\mathbf{x}), \Phi(\mathbf{x}))\right] \qquad (16.59)$$

The calculation is done at fixed temperature. Therefore the resummed effective Lagrangian derived in Sections 9.3 and 15.4 can be used. This is a beautiful example of the use of the effective resummed theory. To lowest order, this means that the coupling constant and the Higgs condensate become functions of temperature, $g(T)$, $v(T)$. Before describing the relevant classical solution to the field equations, let us understand the connection between baryon (and lepton) number violation and the Adler–Bell–Jackiw anomaly. Here we follow Klinkhamer and Manton [24], who coined the word *sphaleron* to refer to this and related classical solutions.

We compute the time rate of change of total baryon number as $dB/dt = \int d^3x \partial J_B^0/\partial t$. Let us assume that either the spatial baryon current $\mathbf{J}_B$ vanishes at spatial infinity or that it is periodic in a large box of volume V. In either case Gauss's theorem can be used to express the volume integral of the divergence of the spatial current in terms of a surface integral, which vanishes under the above assumptions. The change in the baryon number, relative to its value as $t \to -\infty$, is associated with the baryon number of the sphaleron,

$$B_{\text{sphaleron}} = \frac{N_{\text{fam}}g^2}{64\pi^2} \int_{-\infty}^{t} dt' \int d^3x \; \epsilon^{\mu\nu\rho\sigma} f_{\mu\nu}^a f_{\rho\sigma}^a \qquad (16.60)$$

The integrand can be expressed as the divergence of a current:

$$\begin{aligned} \partial_\mu K^\mu &= \frac{1}{2}\epsilon^{\mu\nu\rho\sigma} f_{\mu\nu}^a f_{\rho\sigma}^a \\ K^\mu &= \epsilon^{\mu\nu\rho\sigma}\left(f_{\nu\rho}^a A_\sigma^a - \frac{2}{3}\epsilon_{abc}A_\nu^a A_\rho^b A_\sigma^c \right) \end{aligned} \qquad (16.61)$$

This can be proven by using the classical equations of motion.

To proceed we must have time-dependent fields with finite energy at all times. Furthermore, we want these fields to evolve from the trivial vacuum, $A_\mu^a = 0$, at $t \to -\infty$ to the sphaleron configuration at time t. Moreover, we want A_μ^a to be a pure gauge field at spatial infinity such that $\mathbf{K} = \mathbf{0}$ there. Then we can write

$$B_{\text{sphaleron}} = \frac{N_{\text{fam}}g^2}{32\pi^2} \int d^3x \; K^0(\mathbf{x}, t) \qquad (16.62)$$

Whether this is nonzero depends on the field configuration. Notice that the sphaleron configuration we discussed earlier was time independent. In fact, to make the identification of baryon number with sphaleron, we first find a static configuration of fields and then make a gauge transformation to satisfy the conditions given above.

Define the dimensionless variable $\zeta = gvr$. The static sphaleron ansatz is

$$A^0 = 0$$
$$\mathbf{A} = v\frac{f(\zeta)}{\zeta}\hat{\mathbf{r}} \times \boldsymbol{\sigma} \tag{16.63}$$
$$\Phi = \frac{v}{\sqrt{2}}h(\zeta)\hat{\mathbf{r}} \cdot \boldsymbol{\sigma}\begin{pmatrix} 0 \\ 1 \end{pmatrix}$$

with boundary conditions $f(0) = h(0) = 0$, $f(\infty) = h(\infty) = 1$. The resulting equations of motion are

$$\zeta^2 f'' = 2f(1-f)(1-2f) - \frac{\zeta^2}{4}(1-f)h^2 \tag{16.64}$$

$$\zeta^2 h'' = -2\zeta h' + 2(1-f)^2 h - \frac{\lambda}{g^2}(1-h^2)h \tag{16.65}$$

These cannot be solved exactly in closed form, although analytic approximations can be found. Klinkhamer and Manton showed that the resulting free energy is $F_{\text{sphaleron}} = (4\pi v/g)F_0(\lambda/g^2)$. The factor F_0 varies smoothly from 1.566 at $\lambda = 0$ to 2.722 at $\lambda = \infty$, with $F_0(1) = 2.10$. The characteristic size of the sphaleron is found to be $1/gv$ simply from dimensional analysis. Note that the characteristic energy is $4\pi v/g \approx 5$ TeV when the parameters are those appropriate to the vacuum.

In order to compute the baryon number of the sphaleron we must make a gauge transformation. We choose the gauge transformation

$$U(\mathbf{x}) = \exp\left(\frac{i}{2}\Theta(r)\boldsymbol{\sigma}\cdot\mathbf{x}\right) \tag{16.66}$$

with a function $\Theta(r)$ that varies smoothly from 0 to π as r varies from 0 to ∞. The function should be chosen so that $\mathbf{A}$ goes to zero faster than $1/r$ as $r \to \infty$, so that $\mathbf{K}$ does not contribute to the integral yielding the baryon number. In particular

$$A_i^a = \frac{[1 - 2f(gvr)]\cos\Theta(r) - 1}{gr^2}\epsilon_{iab}x_b$$
$$+ \frac{[1 - 2f(gvr)]\sin\Theta(r)}{gr^2}\left(\delta_{ia}r^2 - x_i x_a\right) + \frac{1}{g}\frac{d\Theta}{dr}\frac{x_i x_a}{r^2} \tag{16.67}$$

By using this formula in K^0 it is easy to show that the baryon number of the sphaleron is $B_{\text{sphaleron}} = N_{\text{fam}}/2$. This is reasonable since the sphaleron interpolates between two sectors that differ by baryon number 1 for each family. The same holds true for lepton number.

The rate of sphaleron transitions involves primarily the Boltzmann factor, but for numerical purposes the prefactor is needed too. Calculation of

the prefactor is analogous to that for the nucleation of bubbles in a first-order phase transition, as analyzed in Chapter 13. The first calculation was performed by Arnold and McLerran [25] who found that

$$\Gamma_{\mathrm{sphaleron}} = \frac{\omega_-}{2\pi}(gv)^3 V \mathcal{N}_{\mathrm{tran}} 8\pi^2 \mathcal{N}_{\mathrm{rot}} \left(\frac{gT}{v}\right)^3 \kappa \exp\left(\frac{-F_{\mathrm{sphaleron}}}{T}\right) \tag{16.68}$$

Here ω_- is the magnitude of the negative mode causing the instability. It was estimated to be of order gv. The volume of phase space associated with translational zero modes is $(gv)^3 V$, where the volume of the box or universe is V. The volume of rotation space, SO(3), is $8\pi^2$. The factors $\mathcal{N}_{\mathrm{tran}}$ and $\mathcal{N}_{\mathrm{rot}}$ relate to the normalization. They are given as integrals involving the functions f and h describing the sphaleron. Finally there is a determinantal factor κ (not to be confused with the quantity used in Chapter 13), that depends on the ratio λ/g^2. It is this last quantity that is very difficult to compute; this must be done numerically with great care. Carson *et al.* [26] found that $\mathcal{N}_{\mathrm{tran}}$ is a smoothly increasing function, and $\mathcal{N}_{\mathrm{rot}}$ a smoothly decreasing function, of λ/g^2. However, their product has the approximately constant value 90 for $0.1 < \lambda/g^2 < 10$. They found that ω_- is a slowly increasing function of the same ratio of couplings and differs from gv by only 30% as λ/g^2 varies by two orders of magnitude. They calculated κ for four different values of λ/g^2. Baacke and Junker [27] also calculated κ for seven values of λ/g^2. Their results are in approximate numerical agreement. It turns out that κ peaks at $\lambda/g^2 \approx 0.4$ and falls off rapidly for both smaller and larger values of λ/g^2. A simple parametrization that captures this feature is

$$\ln\kappa = \ln\kappa_{\mathrm{max}} - 0.09\left(\frac{\lambda}{g^2} - 0.4\right)^2 - 0.13\left(\frac{g^2}{\lambda} - 2.5\right)^2 \tag{16.69}$$
$$\ln\kappa_{\mathrm{max}} = -3$$

If we now put everything together we find the rate per unit volume,

$$\frac{\Gamma_{\mathrm{sphaleron}}}{V} = 56.3\, gv(g^2 T)^3 \frac{\kappa(\lambda/g^2)}{\kappa_{\mathrm{max}}} \exp\left(-\frac{4\pi v}{gT} F_0(\lambda/g^2)\right) \tag{16.70}$$

This depends on two scales, gv and $g^2 T$, as well as on the ratio of the quartic and gauge couplings.

For what range of temperature is the sphaleron rate formula given above valid? It assumes that the baryon- and lepton-changing transitions are dominated by the sphaleron configuration and that higher excitations are unimportant. This means that on the one hand the argument of the exponential must be larger than unity, or $T < 4\pi v/g$. On the other hand, it assumes that gv provides an infrared cutoff smaller than the temperature,

$gv < T$. Therefore the expected range of validity is

$$gv < T < 4\pi v/g \qquad (16.71)$$

The values of v, λ, and g are those appropriate to T, not the zero-temperature values. Of these, v changes the most rapidly with T, as we saw in Sections 15.2 and 15.3. If we use the vacuum value $g = 0.637$ and 10% of the vacuum value of $v = 246$ GeV, the temperature range is 16 to 480 GeV. This is centered directly on the electroweak energy scale, which suggests that the baryon and lepton numbers of the universe were essentially determined when the universe had that range of temperatures.

To relate the sphaleron rate to the baryon-number-changing rate we follow Arnold and McLerran [25]. Suppose that the universe has different sectors of baryon and lepton number and a sphaleron appears. It is associated with baryon and lepton numbers equal to $N_{\text{fam}}/2$. The change in free energy of the universe when a sphaleron is formed now involves the extra term $(\Delta N_B \mu_B + \Delta N_L \mu_L)/T$; $\Delta N_B = \Delta N_L = \pm N_{\text{fam}}/2$, the sign being determined by whether the sphaleron increases or decreases the baryon and lepton numbers. The difference in the forward and backward rates involves the factor

$$e^{(\mu_B + \mu_L)N_{\text{fam}}/2T} - e^{-(\mu_B + \mu_L)N_{\text{fam}}/2T} \approx (\mu_B + \mu_L)N_{\text{fam}}/T \qquad (16.72)$$

where the last approximate equality follows because the chemical potentials are extremely small (the observed baryon-to-photon ratio is about 10^{-9}). Furthermore, the sphaleron facilitates the transition between two sectors that differ by a baryon number value equal to the number of families N_{fam}. Therefore the baryon-changing rate is

$$\frac{dN_B}{dt} = -N_{\text{fam}}^2 \frac{\mu_B + \mu_L}{T} \Gamma_{\text{sphaleron}} \qquad (16.73)$$

We need to relate the baryon number to the chemical potentials. We allow for a third chemical potential μ_{E} associated with electric charge. Taking three families of fermions, calculating the electric charge density and setting it to zero, and solving for the chemical potentials we find that $\mu_{\text{E}} = (3\mu_L - \mu_B)/8$. Then the densities are

$$\begin{aligned} n_B &= \frac{5\mu_B + \mu_L}{8} T^2 \\ n_L &= \frac{9\mu_L + \mu_B}{8} T^2 \end{aligned} \qquad (16.74)$$

If we further assume that the baryon and lepton numbers of the universe are equal we get $\mu_L = \mu_B/2$ and finally $n_B = (11/16)\mu_B T^2$. Putting this

into the baryon-changing rate we finally get

$$\frac{1}{N_B}\frac{dN_B}{dt} = -1100\frac{\kappa(\lambda/g^2)}{\kappa_{\text{max}}}g^7 v \exp\left(-\frac{4\pi v}{gT}F_0(\lambda/g^2)\right) \qquad (16.75)$$

The absolute baryon number is decreased by sphalerons no matter whether it starts out positive or negative.

The characteristic time for the relaxation of baryon and lepton numbers to their equilibrium value of 0 is just given by the previous equation. This should be compared with the expansion rate of the universe. According to Einstein's equations the scale factor of the universe evolves according to (16.53). For an equation of state corresponding to $N_{\text{dof}} \approx 100$ massless bosonic degrees of freedom the characteristic expansion time scale is found from

$$\frac{1}{R}\frac{dR}{dt} = 1.66\sqrt{N_{\text{dof}}}\frac{T^2}{m_{\text{Planck}}} \qquad (16.76)$$

where $m_{\text{Planck}} = G^{-1/2} = 1.22 \times 10^{19}$ GeV. The baryon-number-changing rate is greater than the expansion rate of the universe for temperatures greater than T_*, that is determined approximately by

$$T_* \ln\left(\frac{v m_{\text{Planck}}}{T_*^2}\right) = \frac{4\pi v F_0}{g} \qquad (16.77)$$

The solution to this equation is approximately given by $T_* = v(T_*)$. Within a factor 2 we can estimate T_* to be about 100 GeV, the electroweak scale, that is within the range of validity of the sphaleron approximation to the baryon-changing rate. We would expect the net baryon and lepton numbers of the universe to be determined somewhere around T_*.

For some range of temperatures above the regime of validity of the sphaleron calculation the baryon- and lepton-number-changing reactions are not expected to be suppressed. When $T > 4\pi v/g$ there is no longer a barrier to these reactions. On dimensional grounds the rate per unit volume is then expected to be $Ag^{10}\ln(1/g^2)T^4$, where A is a constant [28, 29]. This involves a factor $(g^2T)^3$, arising from the spatial volume associated with the scale g^2T, and a factor $g^4\ln(1/g^2)T$ arising from the relaxation time. Since the rate per unit volume grows as T^4 and the particle density grows approximately as T^3, the rate per particle grows as T. This should be compared with the T^2 growth of the expansion rate of the universe. Therefore baryon- and lepton-number-changing processes will be predominant for $T_{**} > T > T_*$; it is left as an exercise for the reader to estimate T_{**}.

One can ask a different question. Is it possible for the net baryon and lepton numbers of the universe to be generated at the electroweak scale? This requires three ingredients: baryon- and lepton-changing processes;

CP violation; and a system out of equilibrium. The first has already been demonstrated in the standard model. CP violation also exists in the standard model, as evidenced by neutral kaon oscillations. The requirement that the universe be out of equilibrium is certainly possible if the standard model has a first-order electroweak phase transition. Much work has been done in this context, but the consensus is that there is no first-order electroweak phase transition in the minimal standard model; see Section 15.4. An extension of the minimal standard model to include extra Higgs bosons generally does allow for a first-order phase transition. There also seems to be a consensus that a second-order phase transition is not sufficient to generate baryon and lepton numbers anywhere near their observed values. What happens beyond the minimal standard model is a topic of much current research.

16.6 Decay of a heavy particle

Presumably there is physics beyond the standard model. This may include grand unified theories (GUT), supersymmetry (SUSY), and string theory. A feature common to all of these is the existence of new particles that have masses well above the electroweak scale of 100 GeV. These particles could have been in thermal and chemical equilibrium in the very early universe when the temperature was comparable with or greater than their masses. Since these particles are not observed today they must have been unstable and have decayed to lighter particles. The methods developed in previous chapters are perfectly adapted to describe the physics of these decays at finite temperature.

Following Weldon [30], consider a very heavy scalar field Φ with mass M that decays into a pair of lighter scalar fields ϕ_a and ϕ_b with masses m_a and m_b ($M > m_a + m_b$). The interaction responsible for the decay is taken to be $\mathcal{L}_{\text{int}} = g_s \Phi \phi_a \phi_b$. The self-energy of the Φ can be computed in the one-loop approximation in the usual way:

$$\Pi(k_0 = i\omega_n, \mathbf{k})$$
$$= -g_s^2 T \sum_{j=-\infty}^{\infty} \int \frac{d^3 p}{(2\pi)^3} \frac{1}{\omega_j^2 + \mathbf{p}^2 + m_a^2} \frac{1}{(\omega_j - \omega_n)^2 + (\mathbf{p} - \mathbf{k})^2 + m_b^2}$$
$$\text{(16.78)}$$

Here ω_n and ω_j are the Matsubara frequencies. After performing the sum the self-energy may be expressed as

$$\Pi(k_0 = i\omega_n, \mathbf{k}) = g_s^2 \int \frac{d^3 p}{(2\pi)^3} \frac{1}{2E_a 2E_b} \left(\frac{1 + n_a + n_b}{k_0 - E_a - E_b} + \frac{n_a - n_b}{k_0 + E_a - E_b} \right.$$
$$\left. + \frac{n_b - n_a}{k_0 - E_a + E_b} - \frac{1 + n_a + n_b}{k_0 + E_a + E_b} \right)$$
$$\text{(16.79)}$$

The energies are $E_a = \sqrt{\mathbf{p}^2 + m_a^2}$ and $E_b = \sqrt{(\mathbf{p} - \mathbf{k})^2 + m_b^2}$, and the n_a and n_b are the Bose–Einstein occupation numbers.

Since the Φ is unstable its self-energy has both real and imaginary parts. The imaginary part is what concerns us most here. As in Section 6.6, we write $k_0 = \omega - i\gamma$ and assume weak damping, $\gamma \ll \omega$. Then it is easy to see that

$$
\begin{aligned}
\operatorname{Im} \Pi(\omega, \mathbf{k}) = -\pi g_s^2 \int & \frac{d^3 p}{(2\pi)^3} \frac{1}{2E_a 2E_b} \\
\times & \{[(1 + n_a)(1 + n_b) - n_a n_b] \\
& \times [\delta(\omega - E_a - E_b) - \delta(\omega + E_a + E_b)] \\
& + [n_a(1 + n_b) - n_b(1 + n_a)] \\
& \times [\delta(\omega + E_a - E_b) - \delta(\omega - E_a + E_b)]\}
\end{aligned}
\tag{16.80}
$$

The product $n_a n_b$ has been added and subtracted in each of the terms to provide a transparent physical interpretation. Under the conditions stated above, the kinematically allowed processes are the decay $\Phi \to \phi_a + \phi_b$ and the formation $\phi_a + \phi_b \to \Phi$. The former involves the factor $(1 + n_a)(1 + n_b)$, that is a Bose enhancement of the final state. The latter involves the factor $n_a n_b$ and a relative minus sign as is appropriate for a formation reaction. The overall normalization is governed by the decay amplitude g_s times kinematic factors. At zero temperature all the Bose–Einstein occupation numbers go to zero and $\gamma = -\operatorname{Im}\Pi/2\omega$ just represents the in-vacuum decay. The other terms represent processes that are kinematically forbidden in the present situation but could occur under different ones. They include $\Phi + \phi_a \to \phi_b$, $\Phi + \phi_b \to \phi_a$, $\Phi + \phi_a + \phi_b \to 0$, $\phi_a \to \Phi + \phi_b$, $\phi_b \to \Phi + \phi_a$, $0 \to \Phi + \phi_a + \phi_b$.

It may also be possible for the Φ to decay into a fermion–antifermion pair. This could happen via the interaction $\mathcal{L}_{\text{int}} = g_f \bar{\psi}\psi\Phi$. In that case the imaginary part would be

$$
\begin{aligned}
\operatorname{Im} \Pi(\omega, \mathbf{k}) = -2\pi g_f^2 \int & \frac{d^3 p}{(2\pi)^3} \frac{s - 4m_f^2}{2E_a 2E_b} \\
\times & \{[(1 + n_a)(1 + n_b) - n_a n_b] \\
& \times [\delta(\omega - E_a - E_b) - \delta(\omega + E_a + E_b)] \\
& + [n_a(1 + n_b) - n_b(1 + n_a)] \\
& \times [\delta(\omega + E_a - E_b) - \delta(\omega - E_a + E_b)]\}
\end{aligned}
\tag{16.81}
$$

The physical interpretation of these terms is exactly analogous to those for the decay of the Φ into bosons.

The imaginary part due to the coupling to either bosons or fermions can be written in a universal format:

$$
\begin{aligned}
\operatorname{Im}\Pi(\omega,\mathbf{k}) = -\frac{1}{2}\int &\frac{d^3 p_a}{2E_a(2\pi)^3}\frac{d^3 p_b}{2E_b(2\pi)^3}(2\pi)^4 \\
\times \big\{ &\delta^4(k-p_a-p_b)|\mathcal{M}(\Phi \to a+b)|^2 \\
&\times [(1-n_a)(1-n_b)-n_a n_b] \\
&+ \delta^4(k+p_a-p_b)|\mathcal{M}(\Phi+a\to b)|^2 \\
&\times [n_a(1-n_b)-n_b(1-n_a)] \\
&+ \delta^4(k-p_a+p_b)|\mathcal{M}(\Phi+b\to a)|^2 \\
&\times [n_b(1-n_a)-n_a(1-n_b)] \\
&+ \delta^4(k+p_a+p_b)|\mathcal{M}(\Phi+a+b\to 0)|^2 \\
&\times [n_a n_b-(1-n_a)(1-n_b)]\big\} \qquad (16.82)
\end{aligned}
$$

Here $\mathcal{M}$ is the corresponding amplitude for a given process, whether for bosons or fermions.

This result is of wide application. It applies to final states involving more than two particles also. It easily generalizes to the decay of vector mesons and to the decay of a heavy fermion in an obvious way.

16.7 Exercises

16.1 Derive the formulas for the asymptotic mass and radius of a white dwarf star given in Section 16.1.

16.2 Derive the expression for the charge symmetry coefficient (16.22) given in Section 16.2.

16.3 Using the numbers given in the text, calculate the mean field potential at nuclear saturation density for nucleons and for the Λ, Σ, and Ξ hyperons.

16.4 Calculate the neutrino emissivity for an ultrarelativistic degenerate electron gas ($\mu_e \gg T \gg m_e$).

16.5 Show that the formulas for Z_{T} and Z_{L}, (16.35), (16.36), follow from the previous formulae.

16.6 Look up the relevant matrix element and use it to calculate (16.44).

16.7 Derive formulae for and plot the temperature $T(R)$ and hadronic volume fraction $h(R)$ assuming an idealized Maxwell construction for a QCD phase transition in the early universe.

16.8 Derive the equations of motion for f and h that start from the sphaleron ansatz (16.63).

16.9 Show that the baryon number of a sphaleron is $N_{\mathrm{fam}}/2$ by using (16.67).

16.10 Derive the formulae (16.74) for the baryon and lepton densities.

16.11 Suppose that the baryon-changing rate is given by $Ag^{10}\ln(1/g^2)\,T^4$. If the baryon-to-photon ratio η has the value 10^{-9} at $T = 100$ GeV, what would it have been at earlier times and temperatures? What is your estimate for the temperature T_{**} discussed in the text?

16.12 Consider a very heavy boson of mass M that decays into a massless fermion–antifermion pair. Write down the rate equation for the abundance of these heavy bosons. Solve this equation in the temperature range $M \gg T_0 > T > 100$ GeV in terms of the initial density $n_M(T_0)$.

References

1. Chandrasekhar, S., *Astrophys. J.* **74**, 81 (1931); *Mon. Not. Roy. Astron. Soc.* **95**, 207 (1935).
2. Rufa, M., Stöcker, H., Maruhn, J. A., Greiner, W., and Reinhard, P. G., *J. Phys. G* **13**, L143 (1987).
3. Keil, C. M., Hofmann, F., and Lenske, H., *Phys. Rev. C* **61**, 064309 (2000).
4. Maessen, P. M. M., Rijken, Th. A., and de Swart, J. J., *Phys. Rev. C* **40**, 2226 (1989).
5. Braaten, E., and Segel, D., *Phys. Rev. D* **48**, 1478 (1993).
6. Gamow, G., and Schoenberg, M., *Phys. Rev.* **59**, 539 (1941).
7. Yakovlev, D. G., Kaminker, A. D., Gnedin, O. Y., and Haensel, P., *Phys. Rep.* **354**, 1 (2001).
8. Iwamoto, N., *Phys. Rev. Lett.* **44**, 1637 (1980); *Phys. Rev. D* **28**, 2353 (1983).
9. Burrows, A., *Phys. Rev. D* **20**, 1816 (1979).
10. Witten, E., *Phys. Rev. D* **30**, 272 (1984).
11. Applegate, J. H., Hogan, C. J., and Scherrer, R. J., *Phys. Rev. D* **35**, 1151 (1987).
12. Alcock, C., Fuller, G. M., and Mathews, G. J., *Astrophys. J.* **320**, 439 (1987).
13. Kapusta, J. I., and Olive, K. A., *Phys. Lett.* **B209**, 295 (1988).
14. Kurki-Suonio, H., Matzner, R. A., Olive, K. A., and Schramm, D. N., *Astrophys. J.* **353**, 406 (1990).
15. Kainulainen, K., Kurki-Suonio, H., and Sihvola, E., *Phys. Rev. D* **59**, 083505 (1999).
16. Baym, G., Monien, H., Pethick, C. J., and Ravenhall, D. G., *Phys. Rev. Lett.* **64**, 1867 (1990).
17. Csernai, L. P., and Kapusta, J. I., *Phys. Rev. D* **46**, 1379 (1992).
18. Miller, J. C., and Pantano, O., *Phys. Rev. D* **40**, 1789 (1989); **42**, 3334 (1990).
19. Csernai, L. P., Kapusta, J. I., Kluge, Gy., and Zabrodin, E. E., *Z. Phys. C* **58**, 453 (1993).

20. Bell, J. S., and Jackiw, R., *Nuovo Cimento* **60A**, 47 (1969).
21. Adler, S. L., *Phys. Rev.* **117**, 2426 (1969).
22. 't Hooft, G., *Phys. Rev. Lett.* **37**, 8 (1976); *Phys. Rev. D* **14**, 3432 (1976).
23. Kuzmin, V., Rubakov, V., and Shaposhnikov, M. E., *Phys. Lett.* **B155**, 36 (1985).
24. Klinkhamer, F. R., and Manton, N. S., *Phys. Rev. D* **30**, 2212 (1984).
25. Arnold, P., and McLerran, L., *Phys. Rev. D* **36**, 581 (1987).
26. Carson, L., Li, Xu, McLerran, L., and Wang, R. T., *Phys. Rev. D* **42**, 2127 (1990).
27. Baacke, J., and Junker, S., *Phys. Rev. D* **49**, 2055 (1994); **50**, 4227 (1994).
28. Arnold, P., Son, D., and Yaffe, L. G., *Phys. Rev. D* **55**, 6264 (1997).
29. Bödeker, D., *Phys. Lett.* **B426**, 351 (1998).
30. Weldon, H. A., *Phys. Rev. D* **28**, 2007 (1983).

Bibliography

General relativity

Weinberg, S. (1972). *Gravitation and Cosmology* (Wiley, New York).

Misner, C. W., Thorne, K. S., and Wheeler, J. A. (1973). *Gravitation* (Freeman, San Francisco).

Compact astrophysical objects

Shapiro, S. L., and Teukolsky, S. A. (1983). *Black Holes, White Dwarfs, and Neutron Stars* (Wiley, New York).

Glendenning, N. K. (2000). *Compact Stars*, 2nd edn (Springer, New York).

Newborn neutron stars

Prakash, M., Bombaci, I., Prakash, M., Ellis, P. J., Lattimer, J. M., and Knorren, R., *Phys. Rep.* **280**, 1 (1997).